Appendix to "The absolute instability of an inviscid compound jet"

By Anuj Chauhan, Charles Maldarelli, Demetrios T. Papageorgiou and David S. Rumschitzki

Journal of Fluid Mechanics, vol. 549 (2006), pp. 81—98

Operational notes on the inversion integrals in (29)

Since in the present setting the integrand is explicit in s, it is convenient to consider the alternate, equivalent view of the s-integral as the inner one. The resulting k-integrand is a sum of s-plane residues whose values and character depend on k. This integrand has a number of branch points/cuts, including along the real k-axis, which complicate the process of carrying out the k-integral as a contour integration. In addition, the inner square root in the s-solution has branch points symmetrically placed in each of the four k-plane quadrants, and these branch points are the sources of branch cuts that would render integral closure in the upper half k-plane as branch cut integrations. Instead we opt to handle part of the k-integration directly – for $|k_r|>k_{rc}$ a cutoff value for s-plane residue i, we calculate the long time limit of this part of the integral as zero using the Riemann-Lebesgue lemma (Rudin 1987). Owing to the symmetries of the integrand discussed below, we consider only the portion of the integral $k_{rc}\geq k_r\geq 0$ and carry it out as a contour integration with a contour in the fourth quadrant that avoids the branch cut just described in that quadrant, i.e., closer to the origin than the branch point, when possible. This additional contour Γ begins asymptotically close to the origin (also a branch point) and ends asymptotically close to k_{rc}. If the system contains a source point at $s=\pm i\omega_0$ and if this contour encloses a point k: $s_r(k)=0$, then this point would allow for a change in character of the s-plane residue by virtue of the merging of a pole of |A| with a source pole. As such, if in addition $k_i<0$, it generates a pole in the k-plane that gives rise to a convective instability.

If this contour Γ, which will in general be different for different s-plane residues i

comprising additive terms in the k-plane integrand, can be chosen to pass exclusively through a region having $s_r(k)\leq 0$, then this term does not generate an absolute instability. Figure A.1b, where the portions of both branches [2] and [3] shown derive from the same s-plane residue in the k-integrand, illustrates such a case. Clearly, any curve passing between the curves labeled 0 in the figure will satisfy this criterion. In figure A.1a, the portions of branches [1] and [3] shown derive from different s-plane residues in the k-integrand, and thus need to be handled independently in this matter. Branch [4], not shown, derives from the same s-plane residue in the k-integrand as [1] and lies below and to the right and below the figure. A contour just below the [1] curve labeled 0 and above [4] and above the branch cut (outside of this figure and shown in later figures), is then a valid Γ for this s-plane residue, as is the contour from A.1b for the s-plane residue discussed there. If, on the other hand, there is a point $k^*: k^*_i<0$ and $s_r(k^*)>0$ at which $\partial|A|/\partial k=0$ (equivalent to $ds/dk|_{k^*}$ when $\partial|A|/\partial s\neq 0$), this represents the merger of two branches, e.g., roots [2] and [3] in figure A.2, of the same s-plane residue in the k-integrand. Here root [2] has $s_r>0$ for some k real close to zero and root [3] has $s_r(k)>0$ only for $k_i<0$. The contours for $s_r<s_r(k^*)$, and in particular for $s_r=0$, have a different topology than those for $s_r>s_r(k^*)$ (see figure A.2), so that the region where $s_r<0$ becomes disconnected. As a result the contour Γ must pass through a region in the k plane where $s_r(k)>0$. Let $s^*:=s(k^*)$; as noted $s^*_r>0$. For example, one can integrate across this positive region along a contour (part of Γ), say, of $s_i(k)=s^*_i$ that passes through s^* from one $s_r=0$ branch to the other. If one changes variables from k to s one can see that the resulting integral is equivalent to a branch cut integration in the variable s at the branch point s^*, with the branch cut to the left. This integration leads to a contribution that grows in time proportional to $e^{s_j(k^*)t}/\sqrt{t}$, i.e., it leads to an absolute instability. Figures A.1-A.4, discussed below, search for such points. Thus the mechanics of searching for the possibility of absolute instability by examining the parametrized k-plane plots of $s_r(k)$=constant for decreasing non-negative values of this constant turns out to be the same, irrespective of whether one considers the k-integral or the s-integral as the inner one.

Merging Patterns in the k Plane (The origin of the absolute instability)

In each of the figures A.1-A.4 below, we plot curves that represent the solutions of the

dispersion equation for values of k: $s(k)=s_r-i\omega$; $\omega>0$ parametrizes the curve (see below), i.e., the images k(s) in the k-plane of vertical lines in the s-plane, and the arrows on each curve show the direction of increasing ω. The curves/roots labeled [1], [2] lie in the upper, and those labeled [3], [4] lie in the lower half k plane at large s_r. In the region closer to the origin than the branch cut shown in figures A.3 and A.4, roots [1] and [4] come from one s-plane residue in the k-integrand and roots [2] and [3] from another. On reducing s_r [1], [2] move down and [3], [4] move up and can result in intersections. Upon further reducing s_r, the topology of the continuous branches of the image of the s-plane vertical lines changes and only a part of each continuous branch at lower s_r derive from branches [1] or [2] and part from [3] or [4]. We follow the pattern of mergings and topology changes for V=2.00, 1.75, 1.50, 1.30, 1.00 and 0.50 in table 1 and associated figures. To keep track of the section of each branch which continues to the upper half k plane for large s_r, we denote the frequencies ω (the parameter along the branch curve) for which the root derives from the upper half k plane by ω_u and denote these intervals of ω_u in table1 following the root designation. For example, since the entire root [1] is in the upper half k-plane for large s_r, we write 1, $\omega_u>0$. Similarly, the entire root [3] moves to the lower half for large s_r; hence 3, $\omega_u=\phi$, where ϕ is the null set. The condition for absolute instability implies that ω at the intersection, ω_a, should belong to ω_u for precisely one of the intersecting roots. Also, we label each branch of s_r=constant that results when the constant is just below the s_r value at merging by a combination of the labels of the two branches that merged to form the given branch, with the branch donating the lower ω values first. Many examples follow.

By examining the matrix in equation (26), one can show that the dispersion equation $\phi(s,k;V)=|A|$ satisfies the symmetries $\phi(s,k;V)= \phi (s^*,k^*;-V)^*$ and $\phi (s,k;V)=-[\phi (s^*,-k^*;V)]^*= [\phi (-s^*,k^*;V)]^*$, where * denotes complex conjugate. Thus if $\phi (s_r+i\omega,k_r+ik_i;V)=0$, then $\phi (s_r-i\omega,-k_r+ik_i;V)=0$, or for a given s_r the solution for $s_i=-\omega$ is a mirror image of $s_i=\omega$ about the imaginary k axis. This symmetry permits us to only inspect $\omega>0$, i.e., $s_i<0$. Also, if $s_r=0$, $s^*=-s$. Hence if $\phi(i\omega,k_r+ik_i;V)=0$, then $\phi (i\omega,k_r-ik_i;V)=0$ or, for purely imaginary s, the solutions in the upper and lower half k planes are mirror images.

Figures A.1a,b show three roots of the dispersion equation in the k plane for V=2.0 with

the value of s_r labeling the curves and with ω parametrizing them, where $s=s_r-i\omega$. In these and subsequent figures A.1-A.4, a=2, γ=2 and β=1. At V=2 there is no merging of roots for $s_r \geq 0$. The intersections in the k plane of modes [1] and [3] are not mergings because, as noted, the portions of these roots shown derive from different s_j residues (and so they have different s_i values). Modes [1] and [3] are shown in figure A.1a and modes [2] and [3] in figure A.1b. At s_r=0, modes [1] and [2] join the real k axis, to the right of critical values that, as noted earlier, are close to, but not equal to 1 and 1/a, respectively. They only equal to 1 and 1/a at V=0.

In this paragraph, we consider the presence of a source $F_i(s)$. The s-plane integration in equation 29 would have one or more poles on the imaginary axis, whose residues could contribute convective instability if $k_i<0$ there. Modes [1] and [2] lie totally in the upper half k-plane for sufficiently large s_r and thus inside a contour Γ for the k-plane integration that runs along the real k-axis. Upon decreasing s_r modes [1] and [2] move down and mode [3] moves up. At s_r=0, where the s-plane pole or poles deriving from the forcing function reside, parts of these modes lie in the lower half k-plane, i.e., $k_i(s_r=0)<0$ for these modes, and therefore the corresponding k-integration contour must deform into the lower half plane around them; thus these modes would contribute residues that grow axially in space (Bers 1983; Briggs 1964; Huerre &Monkewitz 1990). Mode [3] is an evanescent mode, i.e., it does not contribute to instability because it lies outside the contour of integration for the Fourier inversion. There is another evanescent mode that will contribute to absolute instability at lower velocities. We call this mode [4] and will show it in later figures. The spatial growth rate $-k_i$ of each convectively unstable mode would change with disturbance frequency ω, with a maximum $k_{i,max}$ for each mode i=1,2. For all frequecies the spatial growth rate of mode [1] is the higher.

On reducing the velocity to 1.75 (see figure A.2 and table 1), root [2] merges with evanescent root [3] at the positive s_r listed in the table. On further reducing s_r, the curves split to form [23] and [32], which are plotted in figure A.2 for s_r=0. Clearly, for any k in the region between [23] and [32] there is at least one solution s(k) for which $s_r>0$. Thus, we choose Γ (not shown) such that between curves [23] and [32] it is the mapping of $s_i=s_{i,m}$=-0.81. Since s_r is positive along at least part of the k_j curve, the e^{st} in the residue of (29) guarantees that this contributes exponential growth in time, i.e., an absolute instability. Root [1] appears in the figure

to illustrate that it has not merged with any evanescent roots.

On further reducing the velocity, more modes becomes absolutely unstable, i.e., either the curve Γ has to pass through two or more regions where $s_r(k)>0$ along it or one must construct different Γ curves for each of the two convectively unstable modes and they both have to pass through regions where $s_r>0$ along Γ.

For V=1.50 (figure not shown; see table 1), roots [2] and [3] again merge. It represents absolute instability, i.e., ω_a belongs to ω_u for root [2] only. On further reducing s_r, the new s_r=constant curves [23] and [32] result. The part of [32] for $\omega_u>0.66$ was in the upper half k and the rest was in the lower half k-plane for large s_r. However, unlike in figure A.2, here a second intersection takes place for $s_r>0$, between [23] and [1] at the value noted in table 1. This also causes absolute instability because $\omega_a=0.69$ belongs to ω_u for mode [1] only. (If ω_a at this second intersection were less than that for the first intersection, ω_a would belong to ω_u for both roots and hence the merger would not cause absolute instability.) This merger takes place just beneath the branch cut (see below) where that part of root [1] derives from the same s-plane residue as the parts of root [2] above the branch cut. It thus still represents a point at which $\partial A/\partial k=0$. The new s_r=constant curves upon reducing s_r are [123] and [231]. There are no further mergers for $s_r>0$.

Figure A.3 and table 1 show the mergings at V=1.30. The first merger takes place between root [1] and root [3], not between roots [2] and [3] as for V=1.50 and 1.75. (Small circles in figures A.3 and A.4 indicate the points of merger.) It represents absolute instability because $\omega_a=0.60$ belongs to ω_u for mode [1] only. On reducing s_r these roots split to form [13] and [31]. The next merger takes place between [31] and [2] at $s_r=0.042$. Note, as was the case for V=1.50 in the last paragraph, this merger takes place below the branch cut (indicated by asterisks) and is thus a point at which $\partial A/\partial k=0$. It also causes absolute instability because $\omega_a=0.56$ belongs to ω_u for [2] only. After splitting these roots form [231] and [312]. On reducing s_r further to 0.017, [231] intersects with [4]. For this merger $\omega_a=1.12$ belongs to ω_u for mode [231] only. Thus, this merger is also absolutely unstable. After the merger the roots split into [2314] and [4231] and no further mergers occur for positive s_r.

At V=1 (figure not shown; see table 1) the merging pattern is again different. There are

three mergings and each one is again absolutely unstable. The first one is between [1] and root [3] at s_r=0.12. It represents absolute instability because ω_a=0.46 belongs to ω_u only for mode [1]. On reducing s_r these roots split to form [13] and [31]. This merger is similar to the one at V=1.30 but the next one is different. It takes place between [31] and [4] at s_r=0.10. It also causes absolute instability because ω_a=0.47 belongs to ω_u for only [31]. After splitting these roots form, [431] and [314]. On reducing s_r further, the third merging occurs at s_r=0.072 between [314] and [2]. ω_a=0.41 belongs to ω_u for mode [2] only. Thus, this merger is also absolutely unstable. After the merger the roots split into [2314] and [3142] (not shown) with no subsequent s>0 mergers.

Figure A.4 and table 1 show the mergings at V=0.50. The first merging is between [1] and root [4] at s_r=0.24. It represents absolute instability because ω_a=0.35 belongs to ω_u for mode [1] only. On reducing s_r these roots split to form [14] and [41]. The next merger takes place between [14] and [3] at s_r=0.22. It also causes absolute instability because ω_a=0.25 belongs to ω_u for [41] only. After splitting the s_r=0 curves become [314] and [143] On reducing s_r further to 0.12, a third merging between [314] and [2] occurs. ω_a=0.19 belongs to ω_u for mode [2] only. Thus, this merger is also absolutely unstable. After the merger the s_r=constant curves become [3142] and [2314] with no subsequent s>0 mergers.

At V=0.10 (not shown) the first merger is similar to that at V=0.50. There the second merger is between [14], $\omega_u<\omega_{a,1}$ and [3,]$\omega_u=\phi$, where $\omega_{a,1}$=0.35 is the frequency at the first merger. This second merger is absolutely unstable if the frequency $\omega_{a,2}$ at merger lies in the range of ω_u for [14], i.e., $\omega_{a,2}<\omega_{a,1}$. But this is not the case for V=0.10 and hence the second merger does not cause absolute instability here. It results in [314], ϕ and [143], $\omega_u<\omega_{a,1}$. The third merger between [2], $\omega_u>0$ and [314], ϕ (and not [314], $\omega_{a,2}<\omega_u<\omega_{a,1}$ as before) is still absolutely unstable.

At V=0 the merging pattern is the same as at V=0.10. What is unique, however, is that the two mergings (the first and the third) which give rise to absolute instability, i.e., which take place for $s_r>0$, take place on the real k axis. Recall the dispersion equation $s_n+ik_nV=g(k_n)$. At V=0 and k real, $s=g(k_r)$, which is simply the equation for the temporal roots. As noted in the Introduction, the temporal roots are purely real when unstable. The merging of roots requires, in addition, ds/dk= d(g(k))/dk=0 at V=0, which, as stated in the text, is just the condition for the

maximum temporal growth rate.

Supplementary Material Figure Captions

Figure A.1a and A.1b. Curves in the k plane of constant s_r and varying s_i (=-iω) for roots lying in the upper (labeled [1] and [2]) and lower (labeled [3]) k plane for large s_r. The values of s_r on the individual loci are indicated in the figure, and the arrows indicate increasing ω which parametrizes the curves. V=2, a=2, β=1 and γ=2. For V=2, no merging occurs for roots originating in the opposite half-planes for s_r greater or equal to zero.

Figure A.2 Curves in the k plane of constant s_r and varying s_I (=-iω) for roots lying in the upper (labeled [1] and [2]) and lower (labeled [3]) k plane for large s_r. The curves [2] and [3] have merged to form [23] and [32] for a positive value of s_r which then split to form the branches shown for s_r=0. V=1.75, a=2, β=1 and γ=2.

Figure A.3 Curves in the k plane of constant s_r and varying s_I (=-iω) for roots lying in the upper (labeled [1] and [2]) and lower (labeled [3] and [4]) k plane for large s_r. Asterisks represent the branch cut of the integrand and the small circles the points of merger. The curves [1] and [3] merge to form [13] and [31] for a positive value of s_r one of which [31] then further merges with [2] to form [231] and [312] again for positive s_r. The [231] branch then merges with [4] to form [2314] and [4231]. V=1.3, a=2, β=1 and γ=2.

Figure A.4 Curves in the k plane of constant s_r and varying s_I (=-iω) for roots lying in the upper (labeled [1] and [2]) and lower (labeled [3] and [4]) k plane for large s_r. . Asterisks represent the branch cut of the integrand and the small circles the points of merger. The curves [1] and [4] merge to form [14] and [41] for a positive value of s_r one of which [14] then further merges with [3] to form [143] and [314] again for positive s_r. The [314] branch then merges with [2] to form [3142] and [2314]. V=.5, a=2, β=1 and γ=2.

Acknowledgments

We thank Air Force Office for Scientific Research (F49620-94-1-0242 to DP), National Science Foundation (DMS 9-9-0070 to DP, CTS 8658147 to DR) and the donors of the Petroleum Research Fund (ACS-PRF #27403-AC9 to DR) for supporting this work. Additional support for DTP was provided by the National Aeronautics and Space Administration under Contract No. NAS1-19480 while the author was in residence at the Institute for Computer Applications in Science and Engineering (ICASE), NASA Langley Research Center, Hampton, VA 23681-0001. DR would also like to thank the Alexander von Humboldt Foundation for providing fellowship support at the Ruhr University of Bochum, where a portion of this work was done.

Table 1: Summary of merging patterns for decreasing non-dimensional velocities V

V	s at merg-ing	k at merg-ing	merging roots	merg ing root s	post merging roots	post merging roots	ω_u	figure number
2.00	none	none	none	none	none	none	none	A.1a,b
1.75	0.0008 -0.81i	0.61-.041i	2, $\omega_u>0$	3, $\omega_u=\phi$	23, $\omega_u<0.81$	32, $\omega_u>0.81$	0.81	A.2
1.50	.021-0.66i	0.54-0.10i	2, $\omega_u>0$	3, $\omega_u=\phi$	23, $\omega_u<0.66$	32, $\omega_u>0.66$	0.66	not shown
	0.0044 -0.69i	0.47-0.22i	23, $\omega_u<0.66$	1, $\omega_u>0$	123, $\omega_u<0.69$	231, $\omega_u<0.66$, $\omega_u>0.69$	0.69	not shown
1.30	0.049-0.60i	0.46-0.22i	1, $\omega_u>0$	3, $\omega_u=\phi$	13, $\omega_u<0.60$	31, $\omega_u>0.60$	0.60	A.3
	0.042-0.56i	0.51-0.10i	31, $\omega_u>0.60$	2, $\omega_u>0$	312, $\omega_u>0.56$	231, $\omega_u<0.56$, $\omega_u>0.60$	0.56	A.3
	0.017-1.12i	1.21-0.22i	231, $\omega_u<0.56$ $\omega_u>0.60$	4, $\omega_u=\phi$	2314, $\omega_u<0.56$, $0.60<\omega_u<1.12$	4231, $\omega_u>1.12$	1.12	A.3
1.00	0.11-0.46i	0.44-0.218i	1, $\omega_u>0$	3, $\omega_u=\phi$	13, $\omega_u<0.46$	31, $\omega_u>0.46$	0.46	not shown
	0.10-0.47i	1.00-0.219i	31, $\omega_u>0.46$	4, $\omega_u=\phi$	314, $0.46<\omega_u<0.47$	431, $\omega_u>0.47$	0.47	not shown
	0.072-0.41i	0.47-0.099i	314, $0.46<\omega_u<0.47$	2, $\omega_u>0$	3142, $\omega_u>0.41$	2314, $\omega_u<0.41$, $0.46<\omega_u<0.47$	0.41	not shown
0.50	0.24-0.35i	0.78-0.22i	1, $\omega_u>0$	4, $\omega_u=\phi$	14, $\omega_u<0.35$	41, $\omega_u>0.35$	0.35	A.4
	0.22-0.25i	0.43-0.18i	14, $\omega_u<0.35$	3, $\omega_u=\phi$	143, $\omega_u<0.25$	314, $0.25<\omega_u<0.35$	0.25	A.4
	0.12-0.19i	0.41-0.75i	314, $0.25<\omega_u<0.35$	2, $\omega_u>0$	3142, $\omega_u>0.19$	2314, $\omega_u<0.19$, $0.25<\omega_u<0.35$	0.19	A.4

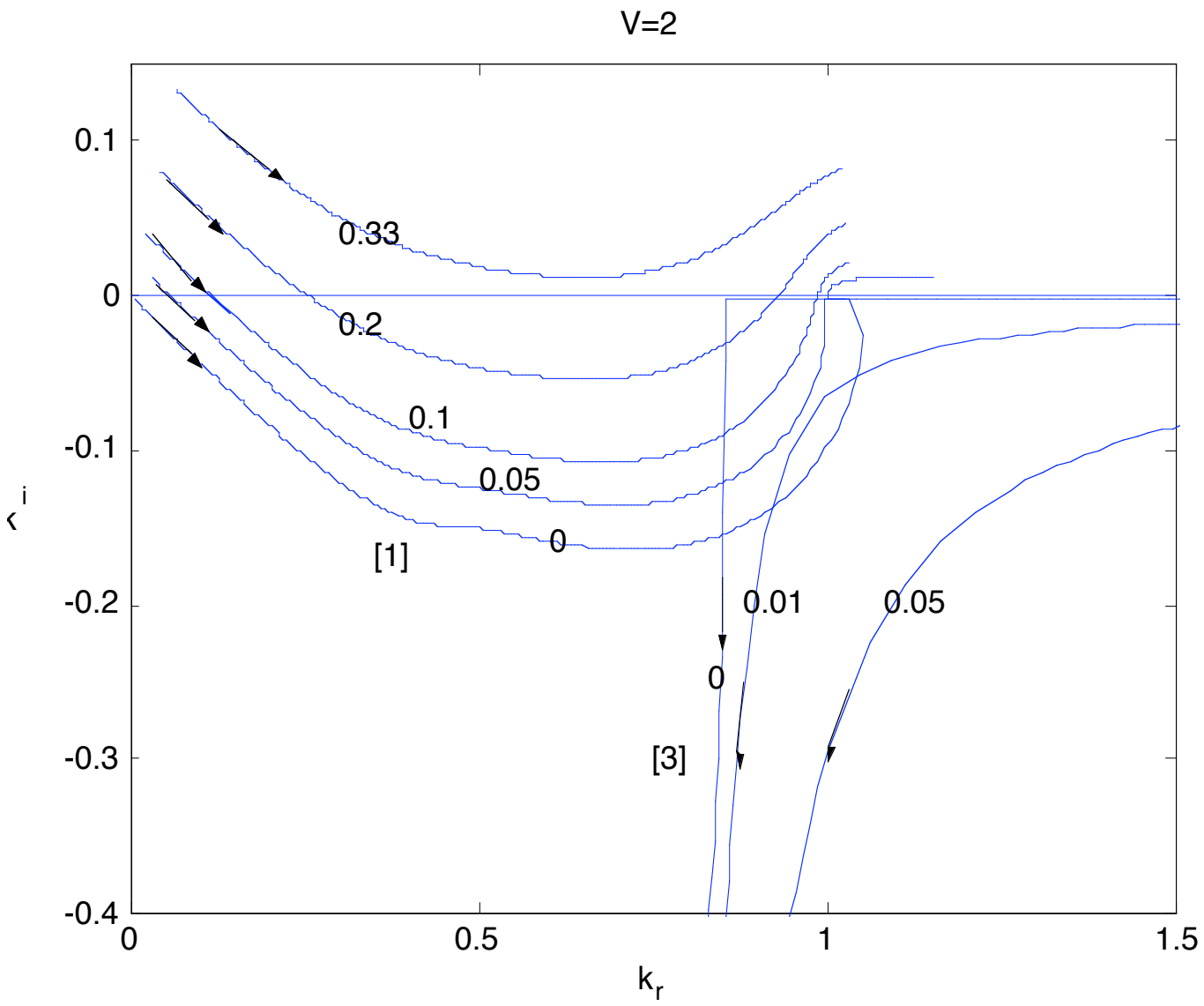

Fig. A1a

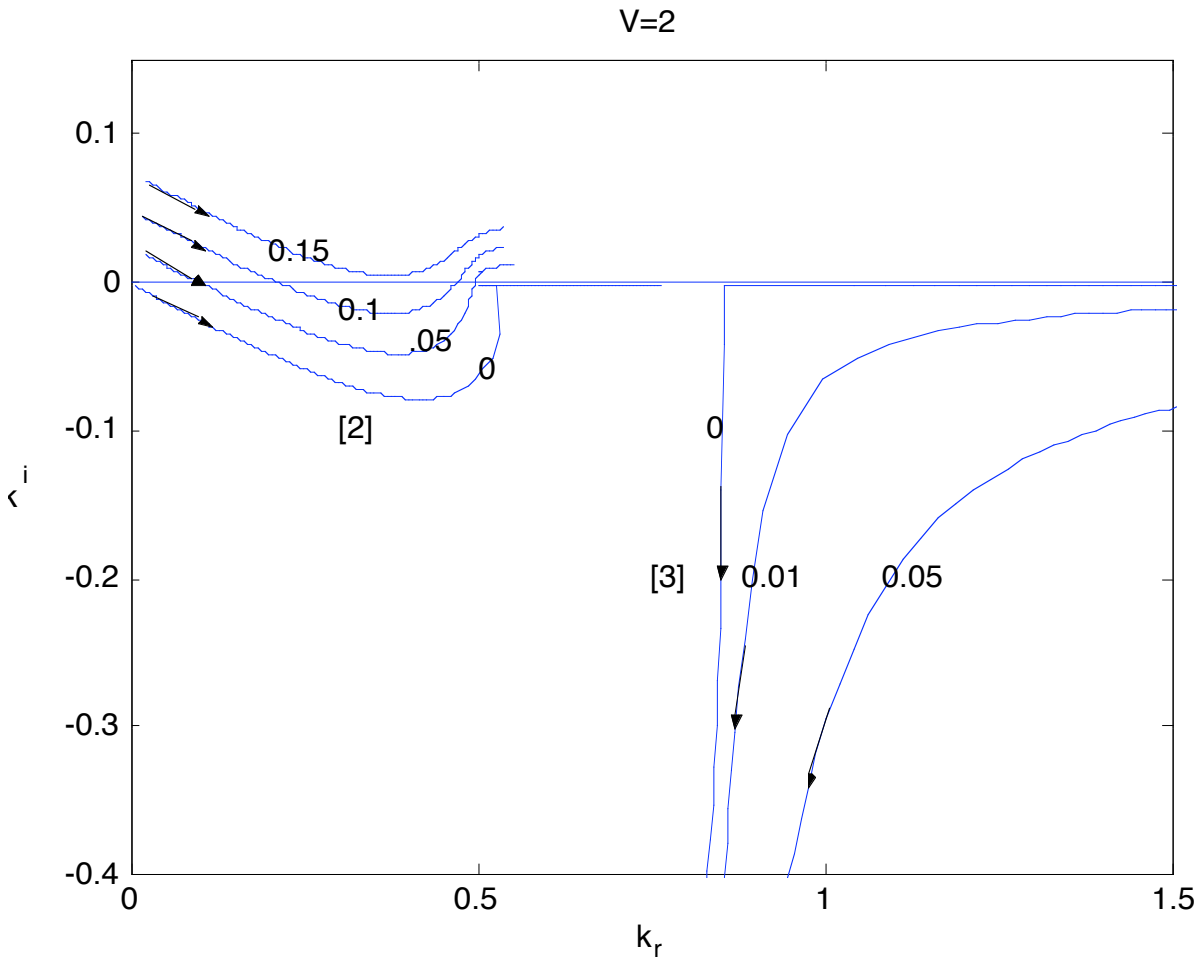

Fig. A1b

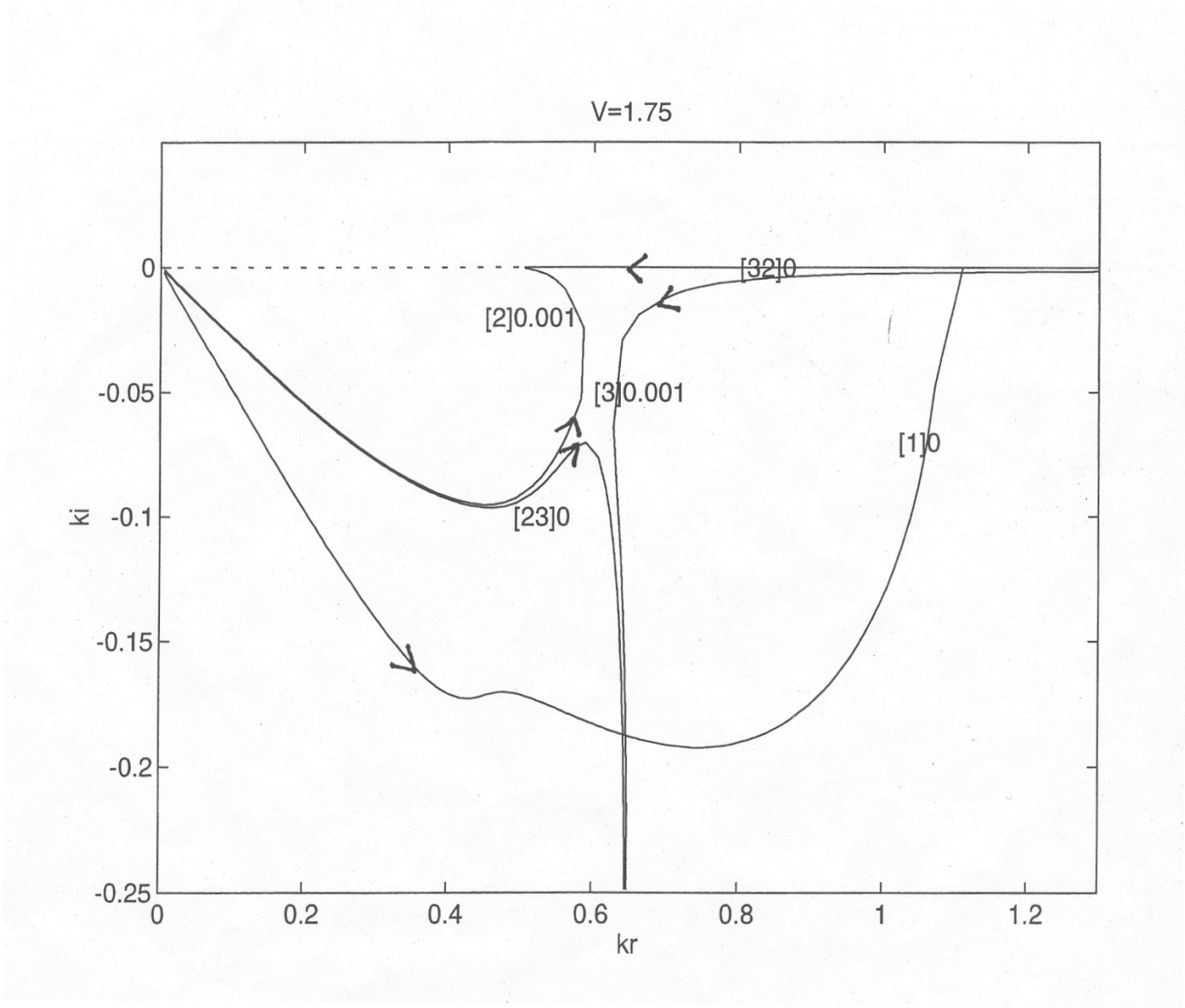
V=1.75
0
-0.05
-0.1
-0.15
-0.2
-0.25
ki
0
0.2
0.4
0.6
0.8
1
1.2
kr
[32]0
[2]0.001
[3]0.001
[1]0
[23]0

Fig. A2

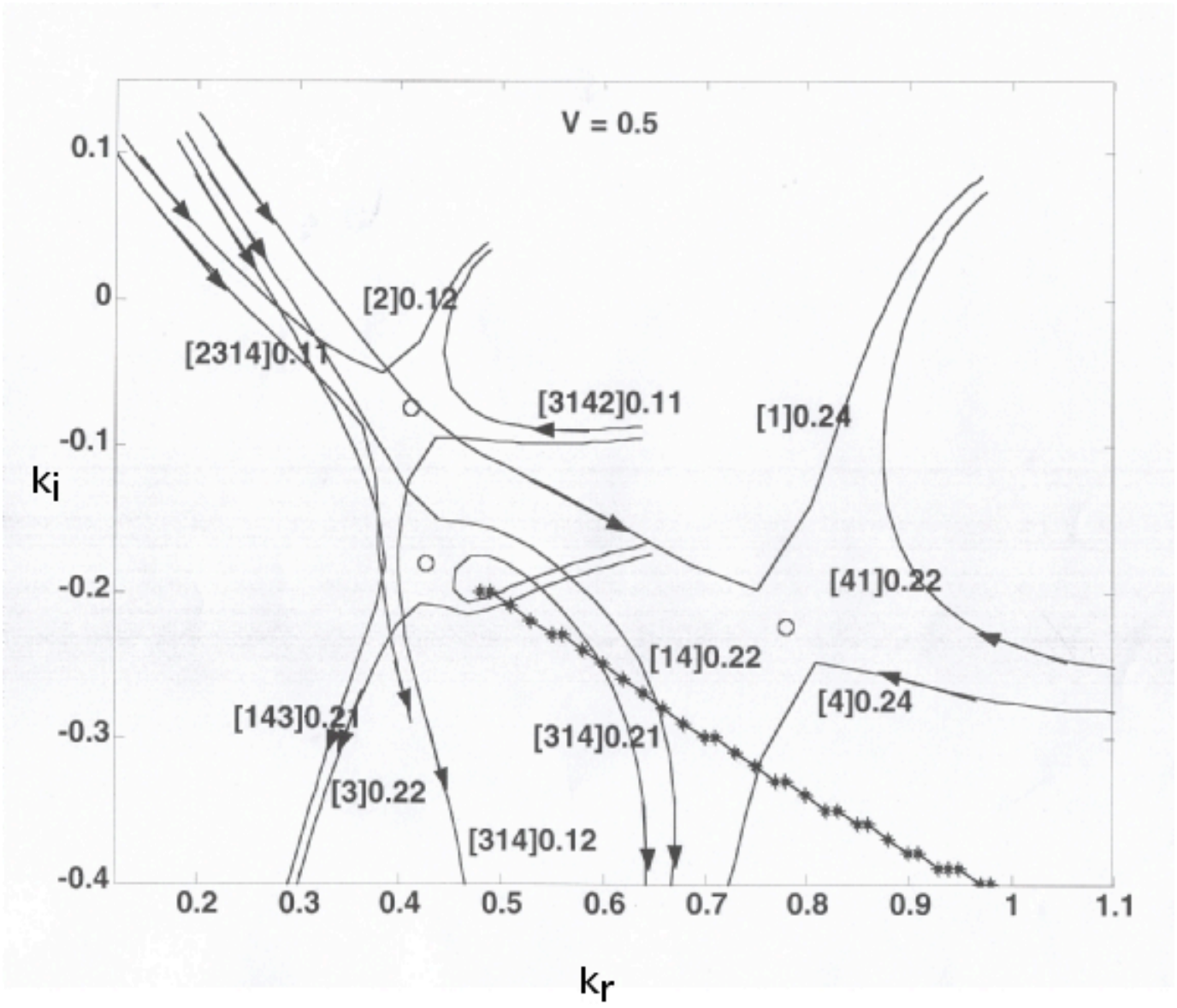
V = 0.5
0.1
0
-0.1
-0.2
-0.3
-0.4
k_i
0.2
0.3
0.4
0.5
0.6
0.7
0.8
0.9
1
1.1
k_r
[2]0.12
[2314]0.11
[3142]0.11
[1]0.24
[41]0.22
[14]0.22
[4]0.24
[143]0.21
[314]0.21
[3]0.22
[314]0.12

Fig. A3

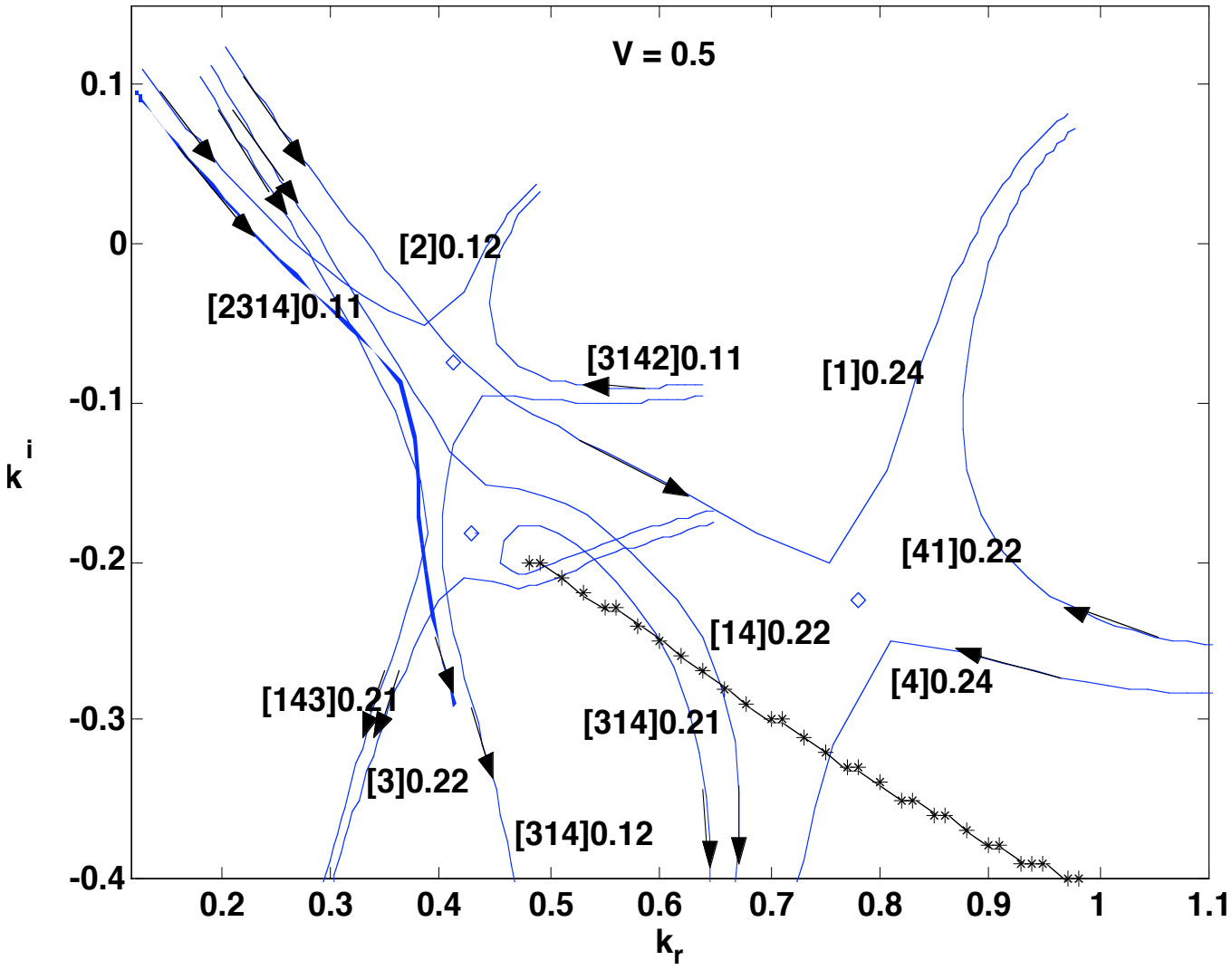
V = 0.5
[2]0.12
[2314]0.11
[3142]0.11
[1]0.24
[41]0.22
[14]0.22
[4]0.24
[143]0.21
[314]0.21
[3]0.22
[314]0.12
k i
k r
0.1
0
-0.1
-0.2
-0.3
-0.4
0.2
0.3
0.4
0.5
0.6
0.7
0.8
0.9
1
1.1

Fig. A3

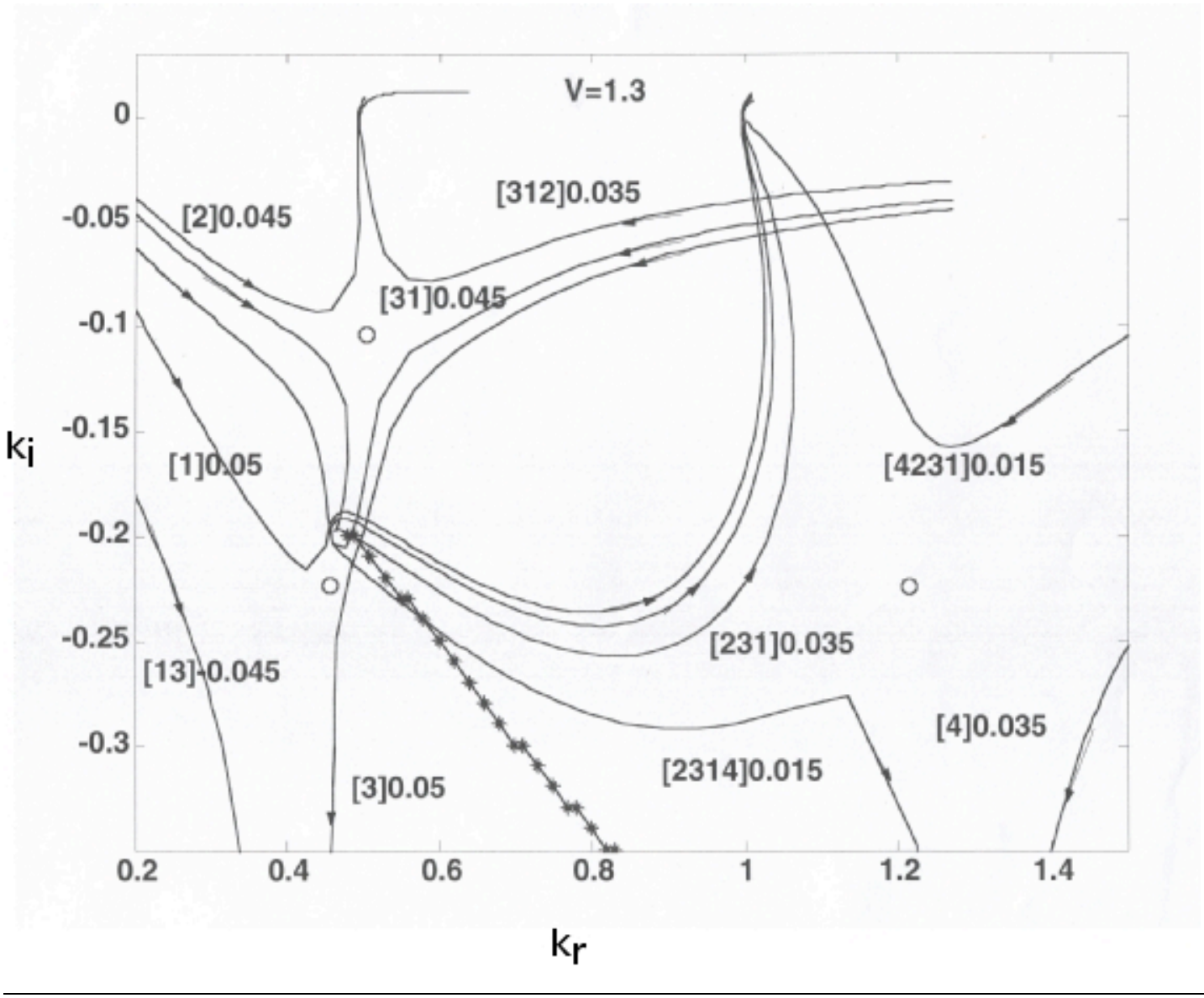
V=1.3
[2]0.045
[312]0.035
[31]0.045
[1]0.05
[4231]0.015
[231]0.035
[13]-0.045
[4]0.035
[2314]0.015
[3]0.05
0
-0.05
-0.1
-0.15
-0.2
-0.25
-0.3
0.2
0.4
0.6
0.8
1
1.2
1.4
ki
kr

Fig. A4